Sensors and Materials, Vol. 31, No. 2 (2019) 501–507
MYU Tokyo

S & M 1790

Structural and Electrical Characteristics of Solution-processed Copper Oxide Films for Application in Thin-film Transistors

Heonju Lee,[1] Xue Zhang,[1] Eui-Jik Kim,[2] and Jaehoon Park[1,2*]

[1]Department of Electronic Engineering, Hallym University,
1 Hallymdaehak-gil, Chuncheon 24252, Korea
[2]School of Software, Hallym University,
1 Hallymdaehak-gil, Chuncheon 24252, Korea

(Received October 15, 2018; accepted December 3, 2018)

Keywords: sol-gel process, oxide semiconductor, copper oxide, thermal annealing, thin-film transistor

In this study, we investigated the effect of the annealing time of copper oxide (CuO) on the morphological and chemical characteristics of films and the electrical properties of bottom-gate/top-contact CuO thin-film transistors (TFTs). Thermogravimetric analysis showed that thermal annealing at 600 °C for 30 min and 3 h resulted in the formation of CuO films. The CuO films were analyzed by X-ray diffraction, X-ray photoemission spectroscopy, absorbance determination, and Raman spectroscopy. As the annealing time of the CuO film was increased, the composition of the films changed from $Cu(OH)_2$ to CuO. Considering the overall TFT performance, the optimal annealing time in solution-processed CuO semiconductors was determined to be 3 h. These results suggest that the annealing time is crucial in modulating the chemical characteristics of solution-processed CuO thin films and the TFT performance.

1. Introduction

Over the past few decades, oxide semiconductors have received considerable attention because of their superior electrical conductivity, high optical transparency in the visible range, and excellent electrical conductivity.[1,2] These essential characteristics of oxide semiconductors are highly advantageous for use in electronics and optoelectronics. In particular, oxide-semiconductor-based thin-film transistors (TFTs) are very promising in a wide range of electronic applications, such as electronic memory devices, sensors, and active-matrix displays.[3–5] Most oxide TFTs are based on n-type semiconductors (e.g., ZnO, In_2O_3, ZnInO, ZnSnO, and InGaZnO), but few p-type oxide TFTs have been reported owing to the lack of p-type oxide semiconductors and rigorous fabrication conditions. This is because of the nonideal electronic configuration of p-type oxide semiconductors: the valence band maximum is mainly composed of anisotropic and localized oxygen 2p orbitals, resulting in a large hole effective mass and low mobility. Although high-performance p-type oxide semiconductors are difficult to realize, they are necessary for constructing complementary logic-based circuits, p–n junction devices,

*Corresponding author: e-mail: jaypark@hallym.ac.kr
https://doi.org/10.18494/SAM.2019.2160

ISSN 0914-4935
https://myukk.org/

and oxide-based solar cells.[6] Among p-type semiconducting oxides, copper oxide (CuO) is a promising material owing to its nontoxicity, low cost, and abundance.

Solution processing is a simple, low-cost method for the fabrication of oxide semiconductors. However, this method has one important drawback: the thin-film properties are affected by the annealing temperature. For example, in the case of CuO films, it has been reported that Cu_2O is converted to CuO during annealing at 250 °C.[7] Therefore, it is very important to study the influence of annealing conditions on the properties of CuO films to improve the performance of CuO-based TFTs. In this study, we fabricated CuO thin films using a sol-gel solution process under ambient air conditions with copper(II) acetate hydrate as a precursor. The prepared sol and films were analyzed by thermogravimetry, X-ray photoemission spectroscopy (XPS), X-ray diffraction (XRD), and field-emission scanning electron microscopy (FE-SEM). The performance of the TFTs, in which a copper oxide layer was used as the semiconductor, was investigated by analyzing their output and transfer characteristics. In addition, we use *in situ* Raman spectroscopy to probe the characteristic changes of CuO films.

2. Materials and Methods

The CuO thin films were prepared by the sol-gel spin coating method. The precursor was prepared by dissolving 0.3 M copper(II) acetate hydrate [$Cu(CO_2CH_3)_2H_2O$] in 5 ml of 2-methoxyethanol (CH_3OCH_2CHOH) with 0.6 M monoethanolamine. To obtain a homogeneously mixed precursor solution, the prepared solution was stirred with a rotation speed of approximately 750 rpm on a hotplate at 75 °C for 1 h using a magnetic bar. For the fabrication of CuO-based TFTs with a bottom-gate/top-contact structure, a p-doped silicon substrate with a 100-nm-thick silicon dioxide (SiO_2) dielectric layer was cleaned via sequential ultrasonication in acetone, isopropyl alcohol, and deionized water. The substrate was subsequently treated with an oxygen plasma for 2 min while an RF power of 45 W was applied and the oxygen flow rate was maintained at 9 sccm. This oxygen plasma treatment was indispensable for generating a hydrophilic surface suitable for the interface between the SiO_2 dielectric and CuO semiconductor layers. The precursor solution was filtered using a 0.2 μm polytetrafluoroethylene syringe filter and then spin-coated on the oxygen-plasma-treated substrate at 2000 rpm for 1 min. In order to form the CuO semiconductor layer, the spin-coated film was prebaked on a hotplate at 150 °C for 20 min and then annealed in a furnace at 600 °C for 30 min or 3 h. Finally, 100-nm-thick Au source and drain electrodes were thermally deposited on the semiconductor layer through a shadow mask. The channel width and length of the fabricated TFTs were 800 and 50 μm, respectively.

The chemical characteristics of the CuO films were investigated by XPS (K-Alpha, Thermo Scientific, Waltham, MA, USA), and the crystallographic properties were characterized by XRD (DMAX-2500, Rigaku, Tokyo, Japan). The surface morphologies of the films were examined by FE-SEM (S-4300, Hitachi, Ibaraki, Japan). The electrical characteristics of the TFTs were evaluated using a semiconductor analyzer (4200-SCS, Keithley, Seoul, Korea). Raman spectroscopy (LabRAM HR Evolution, Horiba Scientific, Kyoto, Japan) was performed to analyze the crystal structure of the films.

3. Results and Discussion

Thermogravimetric analysis (TGA) (N-1000, Sinco, Korea) was used to analyze the thermal decomposition processes of the CuO precursor solution. The measurement was carried out by raising the temperature from 25 to 600 °C at a heating rate of 10 °C/min in a nitrogen atmosphere. Figure 1 shows the TGA curve of the precursor solution in this experiment. We can see that the initial large weight loss (>90%) of the precursor solution occurs below 100 °C, this being a result of the evaporation of the solvent and the decomposition of the precursor. In this process, the $Cu(CO_2CH_3)_2H_2O$ solution is hydrolyzed to $Cu(OH)_2$. As the temperature continues to rise, the weight loss gradually slows and becomes constant. This phenomenon is due to the dehydroxylation process of $Cu(OH)_2$ to form CuO. The thermal decomposition of $Cu(OH)_2$ to produce CuO and H_2O takes place at a temperature of approximately 200 °C. Furthermore, the weight loss is observed to be negligible at temperatures above 500 °C. This indicates that an annealing temperature above 500 °C can be used to convert the precursor solution to CuO. On the basis of the result, a thermal annealing process at 600 °C for 30 min or 3 h was adopted to prepare CuO films from the present precursor solution.

To investigate the surface morphology of the CuO films, the precursor sol was spin-coated on a Si substrate and annealed at 600 °C. Figures 2(a) and 2(b) show the FE-SEM images of the surfaces of the CuO thin films prepared by annealing at 600 °C for 30 min and 3 h. It is shown

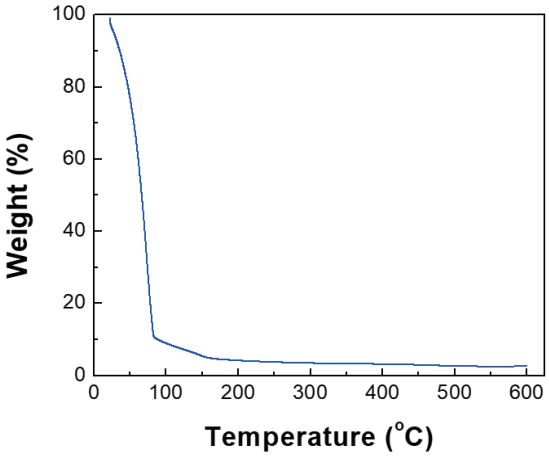

Fig. 1. (Color online) TGA curve of the prepared CuO precursor solution (plot of weight versus temperature).

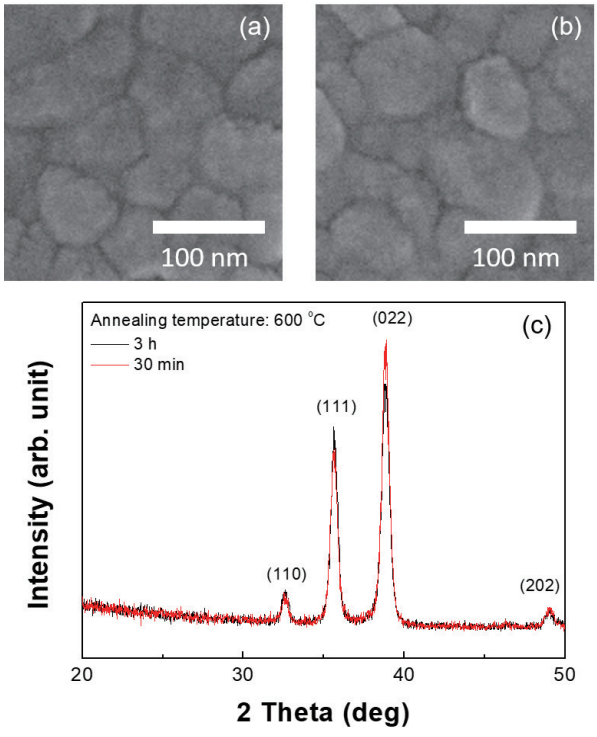

Fig. 2. (Color online) FE-SEM images of CuO thin films annealed at 600 °C for (a) 30 min and (b) 3 h. (c) XRD patterns of the fabricated CuO films.

that the grain sizes of the films are similar regardless of the annealing time. This indicates that crystallite coarsening and condensation phenomena are negligibly affected by the annealing time when the films are thermally treated at 600 °C. Figure 2(c) shows the XRD patterns of the solution-processed CuO films. All the CuO films exhibit diffraction peaks at approximately 32.7, 35.6, 38.9, and 49.0°, which correspond to (110), (002), (111), and (202) planes, respectively.[7] These characteristic peaks can be assigned to the monoclinic symmetry of CuO (space group $C2/c$; a_0 = 4.685 Å, b_0 = 3.423 Å, c_0 = 5.132 Å, β = 99.47°; JCPDS Card no. 48-1548).[8] In particular, the fact that the peak position and width in the XRD spectra for both films are quite similar suggests that there is no marked difference in the crystallinity of the films annealed for different annealing periods in our experiment. This result indicates that crystal growth in the direction of the characteristic peaks is completed within 30 min.

XPS analysis of the CuO films was performed to investigate their chemical characteristics. Each XPS spectrum in Fig. 3 shows two distinct peaks at binding energies of approximately 932 and 952 eV, corresponding to $2p_{3/2}$ and $2p_{1/2}$ states of Cu, respectively. The spin-orbit splitting energy of 20 eV, which is derived from the difference between these two binding energies, is in good agreement with the values reported in the literature.[9] The weak band observed at approximately 940−945 eV corresponds to the shake-up satellite structure. The analysis of Fig. 3 indicates that the Cu 2p peaks are shifted to lower binding energies. According to the literature, the result is attributed to a phase change of Cu from $Cu(OH)_2$ to CuO.[10] Therefore, the performance of the CuO TFTs can be studied on the basis of the difference in the chemical characteristics of the CuO films.

The solution-processed CuO films were also characterized by Raman spectroscopy to analyze the crystal structure of the films. Here, Raman measurements were performed at an excitation wavelength of 532 nm using a conventional Raman spectrometer. Figure 4 shows the Raman spectra of the solution-processed CuO films. Apparently, the obtained Raman spectra of CuO films annealed at 600 °C for different durations seem similar. The CuO film annealed for 30 min exhibits Raman peaks at approximately 293, 340, and 626 cm^{-1}, while the corresponding

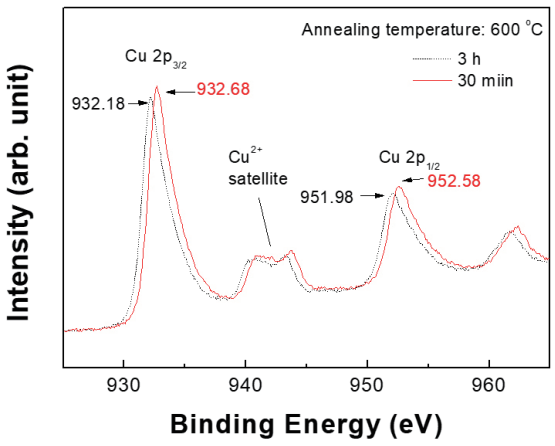

Fig. 3. (Color online) Cu 2p X-ray photoelectron spectra of the fabricated CuO films.

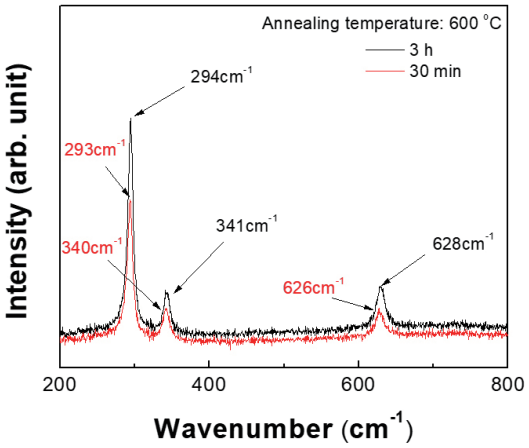

Fig. 4. (Color online) *In situ* Raman spectra of the fabricated CuO films.

Raman peaks in the film annealed for 3 h are observed at approximately 294, 341, and 628 cm^{-1}. Note that the peak at 293/294 cm^{-1} corresponds to the Ag mode and the peaks at 340/341 and 626/628 cm^{-1} correspond to the Bg modes of CuO.[6,11] On the other hand, the shifts in the peak positions towards the high-wavenumber side indicate that the film annealed for 3 h undergoes compression stress during the annealing process. This potentially explains the agglomeration of nanosized crystallites in the CuO film upon thermal annealing for a longer period. It is also an important observation that the full width at half maximum properties of these characteristic peaks tend to be reduced and the peak intensities increase with increasing annealing time. The Raman spectroscopy results reveal that the crystallinity of the solution-processed CuO film can be improved as the annealing time is increased. Therefore, the crystal polymorphism identified by Raman spectra will be significant for understanding the effects of thermal annealing time on the electrical properties of solution-processed CuO TFTs.

To examine the electrical characteristics of the CuO thin films prepared with different annealing durations, bottom-gate/top-contact CuO TFTs were fabricated on SiO_2/Si substrates. Figures 5(a) and 5(b) show the output characteristics of the fabricated TFTs, measured by changing the drain voltage from 0 to −20 V in increments of −1 V at different gate voltages. It is seen from the output characteristic curves that the TFTs exhibit p-channel enhancement mode

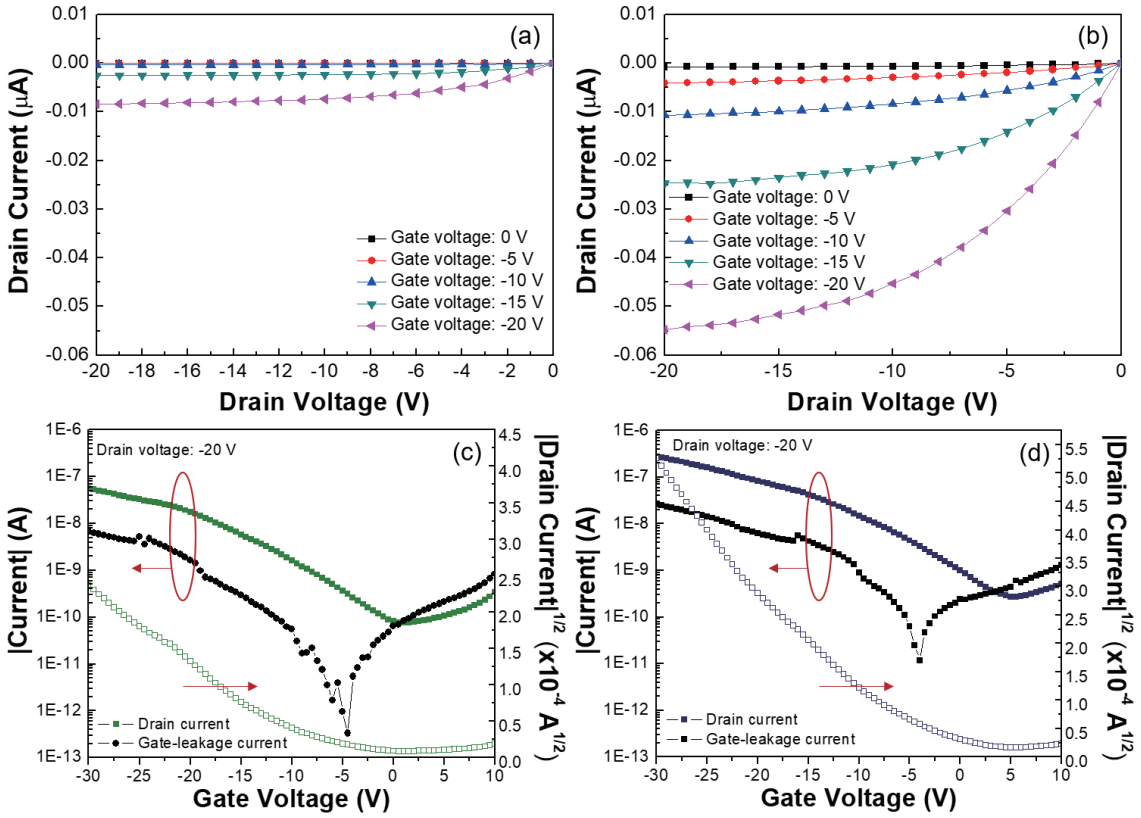

Fig. 5. (Color online) Output and transfer characteristics of TFTs fabricated with CuO films annealed at 600 °C for (a, c) 30 min and (b, d) 3 h.

operation with pinch-off and saturation characteristics of drain currents. Additionally, the drain current is enhanced as the annealing time of the solution-processed CuO films increases.

Figures 5(c) and 5(d) show the transfer characteristics of the fabricated CuO TFTs; the transfer characteristics were measured at a constant drain voltage of −20 V, while the gate voltage was swept from 10 to −30 V in increments of −1 V. In our results, the CuO TFT annealed for 30 min exhibited a field-effect mobility of 4.2×10^{-4} cm^2/Vs, threshold voltage of −8.0 V, and current on/off ratio of approximately 7.3×10^2. Meanwhile, the CuO TFT annealed for 3 h exhibited a field-effect mobility of 1.5×10^{-3} cm^2/Vs, threshold voltage of −4.2 V, and current on/off ratio of approximately 1.0×10^3. As the annealing time was increased, the field-effect mobility increased and the current on/off ratio increased, while the threshold voltage decreased. This can be ascribed to the enhancement of the electrical properties of CuO films owing to the enhancement in the crystallinity shown in Raman results and the reduction of $Cu(OH)_2$ shown in Fig. 3. Taking into account the operation frequency of sensor circuits having a TFT amplifier and a TFT switch, the enhancement in the performance of solution-processed CuO-based TFTs in this study is very promising for realizing high-performance sensors with fast signal processing and sensing capabilities. To further improve the TFT performance in terms of current on/off ratio and field-effect mobility, additional research must be carried out. The results of this study show that increasing the amount of CuO helps to improve the electrical characteristics of solution-processed CuO TFTs. According to the literature, postdeposition annealing under nitrogen atmosphere, postdeposition annealing under oxygen partial pressure, and vacuum annealing help in the generation of CuO.[12–14]

4. Conclusions

We investigated the effects of annealing time on the structural and chemical properties of CuO films and the electrical properties of CuO TFTs. Apparently, the FE-SEM and XRD results showed that the crystallinity of the films annealed at 600 °C is unaffected by the annealing duration as the crystal growth is completed within 30 min. On the other hand, the shift of the Cu 2p peaks in the XPS spectra to lower energies is attributed to the phase transformation of Cu from $Cu(OH)_2$ to CuO. The analysis of the Raman spectra further revealed that the crystalline properties of the solution-processed CuO film improved as the annealing time increased. As the annealing time increased, the drain current and field-effect mobility of solution-processed CuO TFTs increased, but the threshold voltage decreased. The difference in the electrical characteristics of the TFTs with different annealing durations of the solution-processed films is attributed to the formation of CuO. From our results, the optimal annealing duration for a solution-processed CuO semiconductor was found to be 3 h.

The results of this study are useful for analyzing the structural and electrical properties of solution-processed CuO semiconductors in TFT applications. We also believe that these results provide a basis for further studies on the development of high-performance sensors fabricated with solution-processed oxide TFT-based circuits.

Acknowledgments

This work was supported by the Hallym University Research Fund, 2018 (HRF-201805-009).

References

1 T. Minami, H. Nanto, and S. Takata: Appl. Phys. Lett. **41** (1982) 958. https://doi.org/10.1063/1.93355
2 T. Minami: Semicond. Sci. Technol. **20** (2005) S35. https://doi.org/10.1088/0268-1242/20/4/004
3 W. Mi, X. Du, C. Luan, H. Xiao, and J. Ma: RSC Adv. **4** (2014) 30579. https://doi.org/10.1039/C4RA02479F
4 S. Knobelspies, B. Bierer, A. Daus, A. Takabayashi, G. A. Salvatore, G. Cantarella, A. O. Perez, J. Wöllenstein, S. Palzer, and G. Tröster: Sensors **18** (2018) 358. https://doi.org/10.3390/s18020358
5 H. Kim, S. Jeon, M. J. Lee, J. Park, S. Kang, H. S. Choi, C. Park, H. S. Hwang, C. Kim, J. Shin, and U. I. Chung: IEEE Trans. Electron Devices **58** (2011) 3820. https://doi.org/10.1109/TED.2011.2165286
6 Y. Deng, A. D. Handoko, Y. Du, S. Xi, and B. S. Yeo: ACS Catal. **6** (2016) 2473. https://doi.org/10.1021/acscatal.6b00205
7 A. Liu, S. Nie, G. Liu, H. Zhu, C. Zhu, B. Shin, E. Fortunato, R. Martins, and F. Shan: J. Mater. Chem. C **5** (2017) 2524. https://doi.org/10.1039/C7TC00574A
8 B. Zhao, P. Liu, H. Zhuang, Z. Jiao, T. Fang, W. Xu, B. Lu, and Y. Jiang: J. Mater. Chem. A **1** (2013) 367. https://doi.org/10.1039/C2TA00084A
9 Z. H. Gan, G. Q. Yu, B. K. Tay, C. M. Tan, Z. W. Zhao, and Y. Q. Fu: J. Phys. D: Appl. Phys. **37** (2004) 81. https://doi.org/10.1088/0022-3727/37/1/013
10 M. C. Biesinger, L. W. M. Laua, A. R. Gersonb, and R. St. C. Smart: Appl. Surf. Sci. **257** (2010) 887. https://doi.org/10.1016/j.apsusc.2010.07.086
11 M. Rashad, M. Rüsing, G. Berth, K. Lischka, and A. Pawlis: J. Nanomater. **2013** (2013) 714853. http://doi.org/10.1155/2013/714853
12 S. Y. Kim, C, H. Ahn, J. H. Lee, Y. H. Kwon, S. Hwang, J. Y. Lee, and H. K. Cho: ACS Appl. Mater. Interfaces **5** (2013) 2417. https://doi.org/10.1021/am302251s
13 J. Yu, G. Liu, A. Lio, Y. Meng, B. Shin, and F. Shan: Mater. Chem. C **3** (2015) 9509. https://doi.org/10.1039/C5TC02384J
14 Z. Wang, P. K. Nayak, J. A. Caraveo-Frescas, and H. N. Alshareef: Adv. Mater. **28** (2016) 3831. https://doi.org/10.1002/adma.201503080